
Research Articles: Behavioral/Cognitive

Stimulus-driven brain rhythms within the alpha band: The attentional-modulation conundrum

Christian Keitel¹, Anne Keitel^{1,2}, Christopher SY Benwell^{1,2}, Christoph Daube¹, Gregor Thut¹ and Joachim Gross^{1,3}

¹*Institute of Neuroscience and Psychology, University of Glasgow, 62 Hillhead Street, Glasgow G12 8QB, UK*

²*Psychology, School of Social Sciences, University of Dundee, Scrymgeour Building, Dundee DD1 4HN, UK*

³*Institut für Biomagnetismus und Biosignalanalyse, Westfälische Wilhelms-Universität, Malmedyweg 15, 48149 Münster, Germany*

<https://doi.org/10.1523/JNEUROSCI.1633-18.2019>

Received: 29 June 2018

Revised: 16 January 2019

Accepted: 3 February 2019

Published: 19 February 2019

Author contributions: C.K., A.K., C.S.Y.B., C.D., G.T., and J.G. designed research; C.K. and A.K. performed research; C.K. and J.G. contributed unpublished reagents/analytic tools; C.K. and J.G. analyzed data; C.K. wrote the first draft of the paper; C.K., A.K., C.S.Y.B., C.D., G.T., and J.G. edited the paper; C.K., A.K., C.S.Y.B., C.D., G.T., and J.G. wrote the paper.

Conflict of Interest: The authors declare no competing financial interests.

Funded by a Wellcome Trust Joint Investigator Grant awarded to GT and JG (#098433/#098434). Lucy Dewhurst and Jennifer McAllister assisted in data collection. The experimental stimulation was realized using Cogent Graphics (RRID:SCR_015672) developed by John Romaya at the Laboratory of Neurobiology, Wellcome Department of Imaging Neuroscience, University College London (UCL).

Correspondence should be addressed to corresponding author, christian.keitel@glasgow.ac.uk

Cite as: J. Neurosci 2019; 10.1523/JNEUROSCI.1633-18.2019

Alerts: Sign up at www.jneurosci.org/alerts to receive customized email alerts when the fully formatted version of this article is published.

Accepted manuscripts are peer-reviewed but have not been through the copyediting, formatting, or proofreading process.

Copyright © 2019 Keitel et al.

This is an open-access article distributed under the terms of the Creative Commons Attribution 4.0 International license, which permits unrestricted use, distribution and reproduction in any medium provided that the original work is properly attributed.

1 TITLE:

2 **Stimulus-driven brain rhythms within the alpha band: The attentional-modulation conundrum**

3

4 ABBREVIATED TITLE: Reversed attentional modulation of alpha and SSRs

5

AUTHORS:	Affiliation	ORCID	Twitter
Christian Keitel*	1	0000-0003-2597-5499	@KeiCetel
Anne Keitel	1,2	0000-0003-4498-0146	@anneke_sci
Christopher SY Benwell	1,2	0000-0002-4157-4049	@ChrisSYBenwell
Christoph Daube	1	0000-0002-1763-8508	@christophdaube
Gregor Thut	1	0000-0003-1313-4262	
Joachim Gross	1,3	0000-0002-3994-1006	@Joachim__Gross

6

7 AFFILIATIONS:

8 **1** – Institute of Neuroscience and Psychology, University of Glasgow, 62 Hillhead Street, Glasgow
 9 G12 8QB, UK; **2** – Psychology, School of Social Sciences, University of Dundee, Scrymgeour Building,
 10 Dundee DD1 4HN, UK; **3** – Institut für Biomagnetismus und Biosignalanalyse, Westfälische Wilhelms-
 11 Universität, Malmedyweg 15, 48149 Münster, Germany

12 * – corresponding author, christian.keitel@glasgow.ac.uk

13

14 KEYWORDS: alpha rhythm, entrainment, phase synchronisation, spatial attention, steady-state
 15 response (SSR), frequency tagging

16

17 ACKNOWLEDGMENTS: Funded by a Wellcome Trust Joint Investigator Grant awarded to GT and JG
 18 (#098433/#098434). Lucy Dewhurst and Jennifer McAllister assisted in data collection. The
 19 experimental stimulation was realized using Cogent Graphics (RRID:SCR_015672) developed by John
 20 Romaya at the Laboratory of Neurobiology, Wellcome Department of Imaging Neuroscience,
 21 University College London (UCL).

22

0 Table(s), 6 Figure(s), 0 Footnote(s)

23 **ABSTRACT**

24 Two largely independent research lines use rhythmic sensory stimulation to study visual processing.
25 Despite the use of strikingly similar experimental paradigms, they differ crucially in their notion of
26 the stimulus-driven periodic brain responses: One regards them mostly as synchronised (entrained)
27 intrinsic brain rhythms; the other assumes they are predominantly evoked responses (classically
28 termed steady-state responses, or SSRs) that add to the ongoing brain activity. This conceptual
29 difference can produce contradictory predictions about, and interpretations of, experimental
30 outcomes. The effect of spatial attention on brain rhythms in the alpha-band (8 – 13 Hz) is one such
31 instance: alpha-range SSRs have typically been found to *increase* in power when participants focus
32 their spatial attention on laterally presented stimuli, in line with a gain control of the visual evoked
33 response. In nearly identical experiments, retinotopic *decreases* in entrained alpha-band power have
34 been reported, in line with the inhibitory function of intrinsic alpha. Here we reconcile these
35 contradictory findings by showing that they result from a small but far-reaching difference between
36 two common approaches to EEG spectral decomposition. In a new analysis of previously published
37 human EEG data, recorded during bilateral rhythmic visual stimulation, we find the typical SSR gain
38 effect when emphasising stimulus-locked neural activity and the typical retinotopic alpha
39 suppression when focusing on ongoing rhythms. These opposite but parallel effects suggest that
40 spatial attention may bias the neural processing of dynamic visual stimulation via two
41 complementary neural mechanisms.

42 **SIGNIFICANCE STATEMENT**

43 Attending to a visual stimulus strengthens its representation in visual cortex and leads to a
44 retinotopic suppression of spontaneous alpha rhythms. To further investigate this process,
45 researchers often attempt to phase-lock, or entrain, alpha through rhythmic visual stimulation under
46 the assumption that this entrained alpha retains the characteristics of spontaneous alpha. Instead,
47 we show that the part of the brain response that is phase-locked to the visual stimulation *increased*
48 with attention (in line with steady-state evoked potentials), while the typical suppression was only
49 present in non-stimulus-locked alpha activity. The opposite signs of these effects suggest that
50 attentional modulation of dynamic visual stimulation relies on two parallel cortical mechanisms –
51 retinotopic alpha suppression and increased temporal tracking.

52

53 **INTRODUCTION**

54 Cortical visual processing has long been studied using rhythmic sensory stimulation (Adrian and
55 Matthews, 1934; Walter et al., 1946; Regan, 1966). This type of stimulation drives continuous brain
56 responses termed steady-state responses (SSRs) that reflect the temporal periodicities in the
57 stimulation precisely. SSRs allow tracking of individual stimuli in multi-element displays (Vialatte et
58 al., 2010; Norcia et al., 2015). Further, they readily indicate cognitive biases of cortical visual
59 processing, such as the selective allocation of attention (Morgan et al., 1996; Keitel et al., 2013;
60 Stormer et al., 2014).

61 Although SSRs can be driven using a wide range of frequencies (Herrmann, 2001), stimulation at
62 alpha band frequencies (8 – 13 Hz) has stirred particular interest. Alpha rhythms dominate brain
63 activity in occipital visual cortices (Groppe et al., 2013; Keitel and Gross, 2016) and influence
64 perception (Benwell et al., 2017; Iemi et al., 2017; Samaha et al., 2017; Benwell et al., 2018).
65 Researchers have therefore used alpha-rhythmic visual stimulation in attempts to align the phase of
66 – or *entrain* – intrinsic alpha rhythms and consequently provided evidence for visual alpha
67 entrainment (Mathewson et al., 2012; Zauner et al., 2012; Spaak et al., 2014; Gulbinaite et al., 2017).
68 These findings suggest that at least part of the SSR driven by alpha-band stimulation should be
69 attributed to entrained alpha generators (Notbohm et al., 2016).

70 Some issues remain with such an account (Capilla et al., 2011; Keitel et al., 2014). For instance,
71 experiments have consistently reported SSR power increases when probing effects of spatial
72 selective attention on SSRs driven by lateralised hemifield stimuli (Müller et al., 1998a), also when
73 using alpha-band frequencies (Kim et al., 2007; Kashiwase et al., 2012; Keitel et al., 2013). However,
74 recent studies that used similar paradigms, but treated alpha-frequency SSRs as phase-entrained
75 alpha rhythms in line with an earlier study using rhythmic transcranial magnetic stimulation (Herring
76 et al., 2015), reported the opposite effect (Kizuk and Mathewson, 2017; Gulbinaite et al., 2019).
77 Oscillatory brain activity showed attentional modulations characteristic of the intrinsic alpha rhythm
78 during stimulation: Alpha power decreased over the hemisphere contralateral to the attended
79 position, an effect known to be part of a retinotopic alpha power lateralisation during selective
80 spatial attention (Worden et al., 2000; Kelly et al., 2006; Thut et al., 2006; Rihs et al., 2007; Capilla et
81 al., 2012). Briefly put, studies analysing SSRs show a power *increase*, whereas studies analysing
82 “entrained alpha” show a power *decrease* with attention.

83 Both neural responses originate from visual cortices contralateral to the hemifield position of the
84 driving stimuli (Keitel et al., 2013; Spaak et al., 2014). Assuming a single underlying neural process,
85 opposite attention effects therefore seemingly contradict each other. However, results in support of

86 alpha entrainment differed in how exactly responses to the periodic stimulation were quantified.
87 Effects consistent with SSR modulation resulted from spectral decompositions performed on trial-
88 averaged EEG waveforms. This approach tunes the resulting power estimate to the part of the neural
89 response that is sufficiently time-locked to the stimulation (Tallon-Baudry et al., 1996; Delorme and
90 Makeig, 2004). Effects consistent with alpha entrainment instead typically result from averages of
91 single-trial spectral transforms, thus emphasising intrinsic non-phase-locked activity (Tallon-Baudry
92 et al., 1998; Herrmann et al., 2004). Both approaches have been applied before to compare stimulus-
93 evoked and induced brain rhythms in alpha (Moratti et al., 2007) and gamma frequency ranges
94 (~40 Hz; Tallon-Baudry et al., 1998; Picton et al., 2003). Here we focussed on contrasting the
95 attentional modulation of alpha during- and SSRs driven by an alpha-rhythmic stimulation.

96 We therefore compared the outcome of both approaches in a new analysis of previously reported
97 EEG data (Keitel et al., 2017b). Participants viewed two lateralised stimuli, both flickering at alpha
98 band frequencies (10 and 12 Hz). They were cued to focus on one of the two and perform a target
99 detection task at the attended position. We quantified spectral power estimates according to both
100 approaches described above from the same EEG data. Should the outcome depend on the approach
101 taken, we expected to find the typical alpha power lateralisation (contralateral < ipsilateral) when
102 averaging single-trial power spectra. In power spectra of trial-averaged EEG instead we expected the
103 typical SSR power gain modulation in the opposite direction (contralateral > ipsilateral). Crucially,
104 such an outcome would warrant a re-evaluation of stimulus-driven brain rhythms in the alpha range
105 and intrinsic alpha as a unitary phenomenon (alpha entrainment).

106 [Insert Figure 1]

107

108 **METHODS**

109 **Participants**

110 For the present report, we re-analysed EEG data of 17 volunteers recorded in an earlier study (Keitel
111 et al., 2017a). Participants (13 women; median age = 22 yrs, range = 19 – 32 yrs) declared normal or
112 corrected-to-normal vision and no history of neurological diseases or injury. All procedures were
113 approved by the ethics committee of the College of Science & Engineering at the University of
114 Glasgow (application no. 300140020) and adhered to the guidelines for the treatment of human
115 subjects in the Declaration of Helsinki. Volunteers received monetary compensation of £6/h. They
116 gave informed written consent before participating in the experiment. Note that we excluded five
117 additional datasets on grounds reported in the original study (four showed excessive eye
118 movements, one underperformed in the task).

119 **Stimulation**

120 Participants viewed experimental stimuli on a computer screen (refresh rate = 100 frames per sec) at
121 a distance of 0.8 m that displayed a grey background (luminance = 6.5 cd/m²). Small concentric
122 circles in the centre of the screen served as a fixation point (*Figure 1*). Two blurry checkerboard
123 patches (horizontal/vertical diameter = 4° of visual angle) were positioned at an eccentricity of 4.4°
124 from central fixation, one each in the lower left and lower right visual quadrants. Both patches
125 changed contrast rhythmically during trials: Stimulus contrast against the background was modulated
126 by varying patch peak luminance between 7.5 cd/m² (minimum) and 29.1 cd/m² (maximum).

127 On each screen refresh, peak luminance changed incrementally to approach temporally smooth
128 contrast modulations as opposed to a simple on-off flicker (Andersen and Muller, 2015). Further
129 details of the stimulation can be found in Keitel et al. (2017a). The contrast modulation followed a
130 10-Hz periodicity for the left and a 12-Hz periodicity for the right stimulus. Note that the experiment
131 featured further conditions displaying quasi-rhythmic contrast modulations in different frequency
132 bands. Corresponding results can be found in the original report and will not be considered in the
133 present analysis.

134 **Procedure and Task**

135 Participants performed the experiment in an acoustically dampened and electromagnetically
136 shielded chamber. In total, they were presented with 576 experimental trials, subdivided into 8
137 blocks with durations of ~5 min each. Between blocks, participants took self-paced breaks. Prior to
138 the experiment, participants practiced the behavioural task (see below) for at least one block. After
139 each block they received feedback regarding their accuracy and response speed. The experiment was
140 comprised of 8 conditions (= 72 trials each) resulting from a manipulation of the two factors
141 attended position (left vs. right patch) and stimulation frequency (one rhythmic and three quasi-
142 rhythmic conditions) in a fully balanced design. Trials of different conditions were presented in
143 pseudo-random order. As stated above, the present study focussed on the two conditions featuring
144 fully rhythmic stimuli. Corresponding trials ($N = 144$) were thus selected a posteriori from the full
145 design.

146 Single trials began with cueing participants to attend to the left or right stimulus for 0.5 sec, followed
147 by presentation of the dynamically contrast-modulating patches for 3.5 sec (*Figure 1*). After patch
148 offset, an idle period of 0.7 sec allowed participants to blink before the next trial started.

149 To control whether participants maintained a focus of spatial attention, they were instructed to
150 respond to occasional brief “flashes” (0.3 sec) of the cued stimulus (= targets) while ignoring similar

151 events in the other stimulus (= distracters). Targets and distracters occurred in one third of all trials
152 and up to 2 times in one trial with a minimum interval of 0.8 sec between subsequent onsets.
153 Detection was reported as speeded responses to flashes (recorded as space bar presses on a
154 standard keyboard).

155 **Behavioural data recording and analyses**

156 Flash detections were considered a 'hit' when a response occurred from 0.2 to 1 sec after target
157 onset. Delays between target onsets and responses were considered reaction times (RT). Statistical
158 comparisons of mean accuracies (proportion of correct responses to the total number of targets and
159 distracters) and median RTs between experimental conditions were conducted and reported in
160 (2017a). In the present study, we did not consider the behavioural data further. Note that the
161 original statistical analysis found that task performance in Attend-Left and Attend-Right conditions
162 was comparable.

163 **Electrophysiological data recording**

164 EEG was recorded from 128 scalp electrodes and digitally sampled at a rate of 512 Hz using a BioSemi
165 ActiveTwo system (BioSemi, Amsterdam, Netherlands). Scalp electrodes were mounted in an elastic
166 cap and positioned according to an extended 10-20-system (Oostenveld and Praamstra, 2001).
167 Lateral eye movements were monitored with a bipolar outer canthus montage (horizontal electro-
168 oculogram). Vertical eye movements and blinks were monitored with a bipolar montage of
169 electrodes positioned below and above the right eye (vertical electro-oculogram).

170 **Electrophysiological data pre-processing**

171 From continuous data, we extracted epochs of 5 s, starting 1 s before patch onset using the MATLAB
172 (RRID:SCR_001622) toolbox EEGLAB (Delorme and Makeig, 2004)(RRID:SCR_016333). In further pre-
173 processing, we excluded epochs that corresponded to trials containing transient targets and
174 distracters (24 per condition) as well as epochs with horizontal and vertical eye movements
175 exceeding 20 μV ($\sim 2^\circ$ of visual angle) or containing blinks. For treating additional artefacts, such as
176 single noisy electrodes, we applied the 'fully automated statistical thresholding for EEG artefact
177 rejection' (FASTER; Nolan et al., 2010). This procedure corrected or discarded epochs with residual
178 artefacts based on statistical parameters of the data. Artefact correction employed a spherical-
179 spline-based channel interpolation. Epochs with more than 12 artefact-contaminated electrodes
180 were excluded from analysis.

181 From 48 available epochs per condition, we discarded a median of 14 epochs for the Attend-Left
182 conditions and 15 epochs for the Attend-Right conditions per participant with a between-subject

183 range of 6 to 28 (Attend-Left) and 8 to 31 epochs (Attend-Right). Within-subject variation of number
 184 of epochs per condition remained small with a median difference of 3 trials (maximum difference = 9
 185 for one participant).

186 Subsequent analyses were carried out in Fieldtrip (Oostenveld et al., 2011)(RRID:SCR_004849) in
 187 combination with custom-written routines. We extracted segments of 3 s starting 0.5 s after patch
 188 onset from pre-processed artefact-free epochs (5 s). Data prior to stimulation onset (1 s), only
 189 serving to identify eye movements shortly before and during cue presentation, were omitted. To
 190 attenuate the influence of stimulus-onset evoked activity on EEG spectral decomposition, the initial
 191 0.5 s of stimulation were excluded. Lastly, because stimulation ceased after 3.5 s, we also discarded
 192 the final 0.5 s of original epochs.

193 **Electrophysiological data analyses – spectral decomposition**

194 Artefact-free 3-sec epochs were converted to scalp current densities (SCDs), a reference-free
 195 measure of brain electrical activity (Ferree, 2006; Kayser and Tenke, 2015), by means of the spherical
 196 spline method (Perrin et al., 1987) as implemented in Fieldtrip (function *ft_scalpcurrentdensity*,
 197 method 'spline', $\lambda = 10^{-4}$). Detrended (i.e. mean and linear trend removed) SCD time series
 198 were then Tukey-tapered and subjected to Fourier transforms while employing zero-padding in order
 199 to achieve a frequency-resolution of 0.25 Hz. Crucially, from resulting complex Fourier spectra we
 200 calculated two sets of aggregate power spectra with slightly different approaches. First, we
 201 calculated power spectra as the average of squared absolute values of complex Fourier spectra (Z) as
 202 follows:

$$203 \quad onPOW(f) = \frac{1}{n} \sum_{i=1}^n |Z_i(f)|^2 \quad [1]$$

204 where *onPOW* is the classical power estimate for ongoing (intrinsic) oscillatory activity for frequency
 205 f and n is the number of trials. Secondly, we additionally calculated the squared absolute value of the
 206 averaged complex Fourier spectra according to:

$$207 \quad evoPOW(f) = \left| \frac{1}{n} \sum_{i=1}^n Z_i(f) \right|^2 \quad [2]$$

208 The formula yields *evoPOW*, or evoked power, an estimate that is identical with the frequency-
 209 tagging standard approach of averaging per-trial EEG time series before spectral decomposition. This
 210 step is usually performed to retain only the truly phase-locked response to the stimulus (Tallon-
 211 Baudry et al., 1996). Note that both formulas only differ in the order in which weighted sums and
 212 absolute values are computed. Also note that formula [2] is highly similar to the calculation of inter-
 213 trial phase coherence (ITC), a popular measure of phase locking (Cohen, 2014; Gross, 2014; van

214 Diepen and Mazaheri, 2018). ITC calculation additionally includes a trial-by-trial amplitude
215 normalisation. To complement our analysis we thus quantified ITC according to:

$$216 \quad ITC(f) = \left| \frac{1}{n} \sum_{i=1}^n \frac{z_i(f)}{|z_i(f)|} \right| \quad [3]$$

217 For further analyses, power spectra were normalised by converting them to decibel scale, i.e. taking
218 the decadic logarithm, then multiplying by 10 (hereafter termed log power spectra). ITC was
219 converted to ITCz to reduce the bias introduced by differences in trial numbers between conditions
220 (Bonfond and Jensen, 2012; Samaha et al., 2015).

221 **Alpha power – attentional modulation and lateralisation**

222 Spectra of ongoing power (*onPOW*), pooled over both experimental conditions and all electrodes,
223 showed a prominent peak in the alpha frequency range (*Figure 2*). We used mean log ongoing power
224 across the range of 8 – 13 Hz to assess intrinsic alpha power modulations by attention. Analysing
225 Attend-Right and Attend-Left conditions separately, yielded two alpha power topographies for each
226 participant. These were compared by means of cluster-based permutation statistics (Maris and
227 Oostenveld, 2007) using $N = 5000$ random permutations. We clustered data across channel
228 neighbourhoods with an average size of 7.9 channels that were determined by triangulated sensor
229 proximity (function *ft_prepare_neighbours*, method ‘triangulation’). The resulting probabilities (P -
230 values) were corrected for two-sided testing. Subtracting left-lateralised (Attend-Left conditions)
231 from right-lateralised (Attend-Right) alpha power topographies, we found a right-hemispheric
232 positive and a left-hemispheric negative cluster of electrodes that was due to the retinotopic effects
233 of spatial attention on alpha power lateralisation (*Figure 3*), similar to an earlier re-analysis of the
234 other conditions of this experiment (Keitel et al., 2018).

235 Finally, we tested the difference between Attend-Left and Attend-Right conditions, i.e. attention
236 effects for left- and right-hemispheric clusters separately. To this end, we submitted alpha power
237 differences (contralateral hemifield attended minus ignored) to Bayesian one-sample t-tests against
238 zero (Rouder et al., 2009). Attention effects were further compared against each other by means of a
239 Bayesian paired-samples t-test as implemented in JASP (JASP-Team, 2018)(RRID:SCR_015823) with a
240 Cauchy prior scaled to $r = 0.5$, putting more emphasis on smaller effects (Rouder et al., 2012;
241 Schonbrodt and Wagenmakers, 2017).

242 This procedure allowed us to quantify the evidence in favour of the null vs the alternative hypothesis
243 (H_0 vs H_1). For each test, the corresponding Bayes factor (called BF_{10}) showed evidence for H_1
244 (compared to H_0) if it exceeded a value of 3, and no evidence for H_1 if $BF_{10} < 1$, with the intervening
245 range 1 – 3 termed ‘anecdotal evidence’ by convention (Wagenmakers et al., 2011). Inverting BF_{10} , to

246 yield a quantity termed BF_{01} , served to quantify evidence in favour of H_0 on the same scale. For BF_{10}
247 and BF_{01} , values < 1 were taken as inconclusive evidence for either hypothesis. Note that for the sake
248 of brevity we report errors in BF estimates only when exceeding 0.001%.

249 [Insert Figure 2]

250 **SSR power – attentional modulation**

251 Spectra of evoked power, pooled over both experimental conditions and all electrodes, revealed
252 periodic responses to the two stimuli at the respective stimulation frequencies, 10 and 12 Hz
253 (Figure 2). Therefore, we assessed attention effects for these two spectral SSR representations. Two
254 separate cluster-based permutation tests, one for each stimulation frequency, contrasted evoked
255 power topographies between attended and ignored (= other stimulus attended) conditions. Two-
256 sided tests were performed with the same parameters as for alpha power (see above).

257 Again, we found one electrode cluster carrying systematic attention effects per frequency. As for
258 alpha, SSR power from these two clusters were subjected to separate Bayesian one-sample t-tests
259 against zero (one-sided, attended $>$ ignored) and compared against each other by means of a
260 Bayesian paired-sample t-test (two-sided).

261 **SSR inter-trial phase coherence – attentional modulation**

262 We also evaluated a pure measure of neural phase-locking to the stimulation, SSR inter-trial phase
263 coherence (ITC), because evoked power can be regarded as a hybrid measure depending on both the
264 amplitude of the underlying rhythmic response and the consistency of its phase across trials. ITC
265 indicates only the latter as SSRs are set to unit amplitude prior to summing across trials (see
266 formula 3). ITC spectra, pooled over both experimental conditions and all electrodes, showed distinct
267 neural phase-locking at the respective driving frequencies, 10 and 12 Hz (Figure 2). Cluster-based
268 permutation testing confirmed topographic regions that showed systemic gain effects in ITC.
269 Subsequently, the same Bayesian inference was applied to data from these clusters as for SSR power.

270 **Correlation of alpha and SSR attention effects – group level**

271 As a consequence of our counter-intuitive finding that SSR attention effects appeared strongest over
272 occipital regions ipsi-lateral to the driving stimulus (see Results section *SSR power & inter-trial phase*
273 *locking – attentional modulation* below), we explored a posteriori whether these effects could be
274 explained by ipsilateral increases in alpha power during focussed attention. We correlated attention
275 effects on alpha and SSR power using Bayesian inference (rank correlation coefficient Kendall's tau-b
276 or τ_b , beta-prior = 0.75) to test for a positive linear relationship. More specifically, we correlated the
277 left-hemispheric alpha power suppression (Ignored minus Attended) with the 10-Hz SSR (evoked)

278 power attention effect (Attended minus Ignored) and the right-hemispheric alpha power suppression
279 with the 12-Hz SSR power attention effect. We opted for these combinations because the
280 corresponding effects overlapped topographically (see Results). Along with the correlation coefficient
281 ρ , we report its 95%-Credible Interval (95%-CrI).

282 We also probed the linear relationship between alpha power and SSR ITC attention effects. Because
283 ITC gains were not clearly lateralised, we collapsed gain effects (Attended minus Ignored) across both
284 stimulation frequencies and correlated these with a hemisphere-collapsed alpha suppression index.
285 This index was quantified as the halved sum of left and right-hemispheric suppression effects as
286 retrieved from significant clusters in the topographical analysis of alpha power differences (Attend
287 Left minus Attend Right), shown in *Figure 3*. Again, we expected a positive correlation here if alpha
288 power suppression influenced phase-locking to visual stimulation. For means of comparison, we
289 repeated this analysis with attention effects on SSR power collapsed across frequencies.

290 [Insert Figure 3]

291 **Alpha and SSR attention effects – subject level regression**

292 The relationship between alpha power (lateralisation) and SSR attentional modulation was further
293 subjected to a more fine-grained analysis considering within-subject variability across single trials
294 and allowing for a better control of between-subject differences in alpha and SSR power. We
295 assumed that if the SSR attention effect (i.e. the ipsilateral SSR power gain) was a mere consequence
296 of the co-localised alpha power increase then these two effects should co-vary across trials. For this
297 analysis we recalculated single-trial alpha power and SSR evoked power / ITC estimates at each EEG
298 sensor and for both conditions in each subject based on the same artefact-removed EEG epochs and
299 using the same spectral decomposition as described above. Because ITC is not defined for single
300 trials, we used a Jackknife approach that computed single trial estimates in a leave-one-out
301 procedure and allowed for subsequent evaluation of inter-trial variability (Richter et al., 2015). For
302 consistency, we computed similar alpha-power Jackknife estimates. From these estimates, we
303 calculated attention effects as all possible pairwise differences between trials of different conditions
304 (Attend Left vs Attend Right), yielding distributions of alpha power hemispheric lateralisation and SSR
305 evoked power / ITC attentional modulation (for 10 & 12 Hz SSRs separately). To validate this
306 approach, we used it to reproduce alpha power and SSR attention effects described below (data not
307 shown, reproducible via code in online repository (Keitel et al., 2017b)).

308 We then tested for a linear relationship between both z-scored measures by subjecting them to a
309 robust linear regression (MATLAB function 'robustfit', default options), carried out for each EEG
310 sensor separately. The obtained subject-specific regression coefficients θ (slopes) were entered into

311 a group statistical test. We tested slopes against zero (i.e. no linear relationship) by means of cluster-
312 based permutation tests (two-tailed), clustering across EEG sensors. Four tests were carried out in
313 total; one for each regression of alpha power lateralisation with SSR evoked power or SSR ITC
314 attentional modulation, and separately for 10 & 12 Hz SSR, respectively. This procedure was
315 supplemented by sensor-by-sensor Bayesian t-tests (Rouder et al., 2009) to quantify the evidence in
316 favour of a linear vs no relationship (see Methods section *Alpha power – attentional modulation and*
317 *lateralisation* regarding Bayesian inference).

318

319 RESULTS

320 Ongoing alpha power – attentional modulation and lateralisation

321 The power of the ongoing alpha rhythm lateralised with the allocation of spatial attention to left and
322 right stimuli. A topographic map of the differences in alpha power between Attend-Left and Attend-
323 Right conditions shows significant left- and right-hemispheric electrode clusters (*Figure 3*). These
324 clusters signify retinotopic alpha power modulation when participants attended to left vs right
325 stimulus positions (right cluster: $t_{\text{sum}} = -21.454$, $P = 0.026$; left cluster: $t_{\text{sum}} = 81.264$, $P = 0.002$). The
326 differences are further illustrated in power spectra pooled over electrodes of each cluster (*Figure 3*).
327 As predicted, alpha power at each cluster was lower when participants attended to the contralateral
328 stimulus. Bayesian inference confirmed the alpha power attention effect for the right ($M = 0.806$ dB,
329 $SEM = 0.216$; $BF_{10} = 21.17$) and left cluster ($M = 0.790$ dB, $SEM = 0.133$; $BF_{10} = 906.36$). Both effects
330 were of comparable magnitude ($BF_{01} = 4.009 \pm 0.007$).

331 SSR power & inter-trial phase locking – attentional modulation

332 Crucially, we found the opposite pattern when looking at SSRs, i.e. the exact same data but with a
333 slightly different focus on oscillatory brain activity that was time-locked to the stimulation (compare
334 formulas 1 and 2): SSRs showed increased power when the respective driving stimulus was attended
335 versus ignored (*Figure 4*). The power of neural responses evoked by our stimuli (SSRs) was at least
336 one order of magnitude smaller than ongoing alpha power on average (difference > 10dB, i.e.
337 between 10 – 100 times). Nevertheless, SSRs could be clearly identified as distinct peaks in (evoked)
338 power and ITC spectra. Consistent with the retinotopic projection to early visual cortices,
339 topographical distributions of both measures showed a focal maxima contra-lateral to the respective
340 stimulus positions that were attended (*Figure 2*). Counter-intuitively though, maximum attention
341 effects on SSR power did not coincide topographically with sites that showed maximum SSR power
342 overall (compare scalp maps in *Figure 2 & 4*). Also, due to their rather ipsilateral scalp distributions

343 (with respect to the attended location), SSR attention effects did not match topographies of
344 attention-related decreases in ongoing alpha power (compare scalp maps in *Figures 3 & 4*). The 10-
345 Hz SSR driven by the left-hemifield stimulus showed a left-hemispheric power increase when
346 attended ($t_{\text{sum}} = 15.837$, $P = 0.059$). Similarly, attention increased the power of the 12-Hz SSR driven
347 by the right-hemifield stimulus in a right-hemispheric cluster ($t_{\text{sum}} = 53.282$, $P < 0.001$). Bayesian
348 inference confirmed the attention effect on 10-Hz ($M = 3.727$ dB, $SEM = 0.919$; $BF_{10} = 37.05$) and 12-
349 Hz SSR power ($M = 4.473$ dB, $SEM = 0.841$; $BF_{10} = 329.75$) averaged within clusters. Both effects were
350 of comparable magnitude ($BF_{01} = 3.443 \pm 0.005$).

351 SSR phase-locking (quantified as ITCz) also increased with attention to the respective stimulus. In
352 contrast to evoked power, topographical representations of these effects showed greater overlap
353 with the sites that showed maximum phase-locking in general (*Figure 4*). For both frequencies, ITCz
354 increased in central occipital clusters (10 Hz: $t_{\text{sum}} = 41.351$, $P = 0.004$; 12 Hz: $t_{\text{sum}} = 31.116$, $P = 0.012$).
355 Again, Bayesian inference confirmed the attention effect on 10-Hz ($M = 1.386$ au, $SEM = 0.297$;
356 $BF_{10} = 105.71$, one-sided) and 12-Hz ITCz ($M = 1.824$ au, $SEM = 0.451$; $BF_{10} = 36.11$, one-sided).
357 Evidence for a greater attention effect on 12-Hz than on 10-Hz ITC remained inconclusive
358 ($BF_{10} = 0.473$).

359 [Insert Figure 4]

360 **Correlation of alpha and SSR attention effects – group level**

361 Lastly, we tested whether the SSR attention gain effects were mere reflections of the topographically
362 coinciding ipsilateral ongoing alpha power increase during focussed attention that co-occurred with
363 the contralateral ongoing alpha-power decrease (*Figure 3*). Speaking against this account, Bayesian
364 inference provided moderate evidence against the expected positive correlations between the left-
365 hemispheric alpha attention effect and the 10-Hz SSR attention effect ($\tau_b = -0.221$, 95%-CrI = [0.002
366 0.269]; $BF_{01} = 5.811$) and between the right-hemispheric alpha attention effect and the 12-Hz SSR
367 attention effect ($\tau_b = -0.088$, 95%-CrI = [0.004 0.315]; $BF_{01} = 3.904$). These relationships are further
368 illustrated by corresponding linear fits in *Figure 5*.

369 Following this analysis, we further explored the relationship between spatially non-overlapping
370 decreases in alpha-power contralateral to the attended position and the ipsilateral SSR power gain
371 effects. For the lack of a specific hypothesis about the sign of the correlation in this case, we
372 quantified the evidence for any relationship (two-sided test). The results remained inconclusive for a
373 correlation between the left-hemispheric alpha attention effect and the right-hemispheric 12-Hz SSR
374 attention effect ($\tau_b = 0.235$, 95%-CrI = [-0.110 0.487]; $BF_{01} = 1.280$) and between the right-

375 hemispheric alpha attention effect and the left-hemispheric 10-Hz SSR attention effect ($\tau_b = 0.103$,
376 95%-CrI = [-0.218 0.383]; $\text{BF}_{01} = 2.400$).

377 [Insert Figure 5]

378 Finally, we repeated this analysis for attention effects on inter-trial phase coherence (ITC). Because
379 SSR ITC attention effects did not show a clear topographical lateralisation (*Figure 4*), they were
380 collapsed across driving frequencies (10 & 12 Hz). Again, findings were inconclusive when looking
381 into the correlation between these aggregate SSR ITC gain effects and a hemisphere-collapsed alpha
382 suppression index ($\tau_b = -0.059$, 95%-CrI = [-0.349 0.251]; $\text{BF}_{01} = 2.653$). Correlating collapsed attention
383 effects of SSR evoked power with the same pooled alpha suppression index yielded identical results
384 regarding the rank correlation (also see linear fits in *Figure 5*).

385 **Alpha and SSR attention effects – subject level regression**

386 A more fine-grained analysis of single-trial co-variation of alpha power lateralisation and SSR gain
387 effects during focussed spatial attention largely corroborated the group level results. Clustering
388 across EEG sensors, we found that only the 12-Hz SSR evoked power attention effect and alpha
389 lateralisation co-varied systematically across participants at occipital sites (permutation test,
390 $T_{sum} = -17.517$, $p = 0.023$). The negative sign of the slope however contradicted the expected positive
391 relationship (*Figure 6a*). Neither 10-Hz SSR evoked power nor SSR ITC (both frequencies) revealed
392 similar systematic relationships with alpha power.

393 Additionally, we used Bayesian inference on the distributions of individual regression slopes
394 (indicating the linear relationship between alpha and SSR attention effects) by sensor to quantify the
395 plausibility of either H_1 or H_0 in scalp maps (*Figure 6b*). We further overlaid these scalp maps with
396 electrode clusters showing SSR attention effects (compare with *Figure 4*). Average Bayes factors (Bfs)
397 within clusters indicated that evidence for or against any type of linear relationship remained
398 inconclusive for 10-Hz (mean $\text{Bf}_{01} = 1.422$ range = 0.639 – 2.343) and 12-Hz SSR evoked power (mean
399 $\text{Bf}_{01} = 1.245$ range = 0.153 – 3.673), although it should be mentioned that the 12-Hz cluster contained
400 a local maximum ($\text{Bf}_{10} = 1/\text{Bf}_{01} = 6.534$) that coincided topographically with the effect identified by
401 the cluster-based permutation test. For ITC evidence favoured H_0 , i.e. the absence of any relationship
402 with 10-Hz (mean $\text{Bf}_{01} = 3.040$, range = 1.861 – 4.014) and 12-Hz SSR ($\text{Bf}_{01} = 3.030$, range = 1.391 –
403 4.016) was 3 times more likely given our data.

404 Our findings show a fine distinction between SSR evoked power and ITC gain effects with respect to a
405 possible connection to alpha lateralisation in that only the latter provided conclusive evidence
406 against such a relationship. As a likely explanation, SSR evoked power still contains residual alpha

407 activity that confounds tests for covariation. Conversely, the single-trial power normalisation step
408 undertaken during the calculation of SSR ITC makes it less susceptible to this confound. Taken
409 together, the findings of this analysis do not support a positive linear relationship of alpha
410 lateralisation and SSR gain effects (especially on ITC). Therefore, it is unlikely that the counter-
411 intuitive topography of SSR attentional modulation is a reflection of alpha power lateralisation during
412 focused spatial attention.

413 [Insert Figure 6]

414

415 **DISCUSSION**

416 We found that two common spectral measures of alpha-band EEG during alpha-rhythmic visual
417 stimulation reflect effects of spatial attention with opposite signs. In the following we discuss how
418 this finding supports the notion of two complementary neural mechanisms governing the cortical
419 processing of dynamic visual input.

420 **Analysis approach determines sign of attentional modulation**

421 When focussing on the spectral representation of ongoing EEG power, we observed the prototypical
422 broad peak in the alpha frequency range (8 – 13 Hz; *Figure 2*). Moreover, alpha power decreased
423 over the hemisphere contralateral to the attended stimulus position, indicating a functional
424 disinhibition of cortical areas representing task-relevant regions of the visual field (Worden et al.,
425 2000; Kelly et al., 2006; Thut et al., 2006). Concurrently, alpha power increased over the ipsilateral
426 hemisphere, actively suppressing irrelevant and possibly distracting input (Rihs et al., 2007; Capilla et
427 al., 2012).

428 A second approach focussed on the SSRs, i.e. strictly stimulus-locked rhythmic EEG components. As
429 in classical frequency-tagging studies, we found spectrally distinct SSRs at the stimulation frequencies
430 (here 10 and 12 Hz). These two concurrent rhythmic brain responses thus precisely reflected the
431 temporal dynamics of the visual stimulation. Notably, SSR evoked power was between one to two
432 orders of magnitude (10 – 100 times) lower than ongoing-alpha power. Smaller evoked power also
433 explained why SSRs remained invisible in spectra of ongoing activity. They were likely masked by the
434 broad alpha peak (*Figure 2*; Covic et al., 2017). Note that this is a result of the relatively low-intensity
435 stimulation used here. Stimulation of higher intensity can evoke SSRs that are readily visible in power
436 spectra of ongoing activity (Gulbinaite et al., 2019).

437 Crucially, we examined SSRs for effects of focused spatial attention. Visual cortical regions
438 contralateral to the respective driving stimuli showed maximum SSR evoked power. We would

439 expect to observe a decrease in SSR evoked power with attention (Kizuk and Mathewson, 2017;
440 Gulbinaite et al., 2019) under the assumption that SSRs are frequency-specific neural signatures of a
441 local entrainment of intrinsic alpha generators (Spaak et al., 2014; Notbohm et al., 2016) and exhibit
442 similar functional characteristics. Instead, we found that SSR evoked power increased in line with
443 earlier reports (Kim et al., 2007; Kashiwase et al., 2012; Keitel et al., 2013).

444 Note however that these attentional gain effects did not coincide topographically with scalp
445 locations of maximum SSR evoked power (*Figure 4*). Instead, they were most pronounced over
446 hemispheres ipsilateral to the position of the respective driving stimuli and thus co-localised with
447 ipsilateral alpha power increases (*Figure 3*). Two control analyses showed that these effects were
448 unlikely to be related (*Figure 5 & 6*). We have described the apparent counter-intuitive lateralisation
449 of this effect before (Keitel et al., 2017a) when comparing scalp distributions by means of Attended-
450 minus-Unattended contrasts (Keitel et al., 2017a). In that case, expecting attention effects to emerge
451 at sites of maximum SSR power entails the implicit assumption that attention only acts as a local
452 response gain mechanism. Alternatively, neural representations of attended stimuli could access
453 higher order visual processing (Lithari et al., 2016) and a gain in spatial extent could then produce
454 seemingly ipsilateral effects when evaluating topographical differences as observed here. However,
455 previous cortical source reconstructions of SSRs in lateralised stimulus situations have unequivocally
456 localised maximum effects of visuo-spatial attention to contralateral visual cortices (Müller et al.,
457 1998b; Lauritzen et al., 2010; Keitel et al., 2013). Considering the limited spatial resolution of EEG,
458 and that SSR inter-trial phase coherence showed yet another non-lateralised topographical
459 distribution for gain effects (*Figure 4*), warrants a dedicated neuroimaging analysis of the underlying
460 cortical sources that generate these attentional modulations.

461 **Opposite but co-occurring attention effects suggest interplay of distinct attention-related**
462 **processes**

463 Our analysis compared attention effects between “ongoing” spectral power within the alpha
464 frequency band and a quantity termed SSR “evoked power” that is commonly used in frequency
465 tagging research (Colon et al., 2012; Porcu et al., 2013; Stormer et al., 2014; Walter et al., 2016;
466 Martinovic and Andersen, 2018). This term is somewhat misleading because it conflates a power
467 estimate with the consistency of the phase of the SSR across trials of the experiment. Inter-trial
468 phase consistency (ITC) has been used to quantify SSRs before (Ruhnau et al., 2016). It is closely
469 related to evoked power but involves an extra normalisation term that abolishes (or at least greatly
470 attenuates) the power contribution (Cohen, 2014; Gross, 2014). Note that in a noisy, finite signal
471 such as the typical second(s)-long EEG epoch, there will be a positive relationship between the power

472 and inter-trial phase consistency at any frequency as is shown by the greater than zero noise floor in
473 our ITC spectra (Figure 4). Also note that ITC only measures SSRs meaningfully if the
474 neurophysiological signal contains a periodic component at the stimulation frequency.

475 The effects of attention on SSR evoked power and ITC are typically interchangeable (Covic et al.,
476 2017; Keitel et al., 2017a). In fact, increased ITC, or phase synchronisation, has been considered the
477 primary effect of attention on stimulus-driven periodic brain responses (Kim et al., 2007; Kranczioch,
478 2017). Looking at spectral power and ITC separately, as two distinct aspects of rhythmic brain
479 activity, therefore resolves the attentional modulation conundrum: Seemingly opposing attention-
480 related effects likely index different but parallel influences on cortical processing of rhythmic visual
481 input. To avoid confusion, we therefore suggest opting for ITC (or related measures, e.g. the cosine
482 similarity index (Chou and Hsu, 2018)) instead of “evoked power” to evaluate SSRs.

483 Incorporating our findings into an account that regards SSRs primarily as stimulus-driven entrainment
484 of intrinsic alpha rhythms would require demonstrating how a decrease in alpha-band power (i.e. the
485 contralateral alpha suppression) can co-occur with increased SSR phase synchronisation.
486 Alternatively, stimulus-locked (“evoked”) and intrinsic alpha rhythms could be considered distinct
487 processes (Freunberger et al., 2009; Sauseng, 2012). Consequentially, alpha range SSRs could
488 predominantly reflect an early cortical mechanism for the tracking of fluctuations in stimulus-specific
489 visual input per se (Keitel et al., 2017a) without the need to assume entrainment (Capilla et al., 2011;
490 Keitel et al., 2014).

491 The underlying neural mechanism might similarly work for a range of rhythmic and quasi-rhythmic
492 stimuli owing to the fact that visual cortex comprises a manifold of different feature detectors that
493 closely mirror changes along the dimensions of colour, luminance, contrast, spatial frequency and
494 more (Buracas et al., 1998; Blaser et al., 2000; Martinovic and Andersen, 2018). Most importantly, for
495 (quasi-)rhythmic sensory input, attention to the driving stimulus may increase neural phase-locking
496 to the stimulus to allow for enhanced tracking of its dynamics, i.e. increased fidelity. This effect has
497 been observed for quasi-rhythmic low-frequency visual speech signals (Crosse et al., 2015; Park et al.,
498 2016; Hauswald et al., 2018) and task-irrelevant visual stimuli at attended vs ignored spatial locations
499 (Keitel et al., 2017a).

500 Concurrent retinotopic biasing of visual processing through alpha suppression and stronger neural
501 phase-locking to attended stimuli could therefore be regarded as complimentary mechanisms. Both
502 could act to facilitate the processing of behaviourally relevant visual input in parallel. In this context,
503 SSRs would constitute a special case and easy-to-quantify periodic signature of early visual cortices
504 tracking stimulus dynamics over time. Intrinsic alpha suppression instead may gate the access of

505 sensory information to superordinate visual processing stages (Jensen and Mazaheri, 2010; Zumer et
506 al., 2014) and enhanced ipsilateral alpha power may additionally attenuate irrelevant and possibly
507 distracting stimuli at ignored locations (Capilla et al., 2012).

508 A neuronal implementation may work like this: During rest or inattention, occipital neuronal
509 populations synchronise with a strong internal, thalamo-cortical pacemaker (alpha). During attentive
510 processing of sensory input, retinotopic alpha suppression releases specific neuronal sub-populations
511 from an internal reign and allows them to track the stimulus dynamics at attended locations. A
512 related mechanism has been observed in the striatum, where local field potentials are dominated by
513 synchronous oscillatory activity across large areas (Courtemanche et al., 2003). However, during task
514 performance focal neuronal populations were found to disengage from this global synchronicity in a
515 consistent and task-specific manner. At the level of EEG/MEG recordings, such a mechanism could
516 lead to task-related decrease of oscillatory power but increase of coherence or ITC, as observed in
517 the current study and previously in the sensorimotor system (Gross et al., 2005; Schoffelen et al.,
518 2005; Schoffelen et al., 2011).

519 Whereas such an account challenges the occurrence of strictly stimulus-driven alpha entrainment, it
520 may still allow alpha to exert temporally precise top-down influences during predictable and
521 behaviourally relevant rhythmic stimulation – a process that itself could be subject to entrainment
522 (Thut et al., 2011; Nobre et al., 2012; Haegens and Zion Golumbic, 2018; Zoefel et al., 2018).

523 **Conclusion**

524 Our findings reconcile seemingly contradictory findings regarding spatial attention effects on alpha-
525 rhythmic activity, assumed to be entrained by periodic visual stimulation, and SSRs. Focusing on
526 spectral power or phase consistency of the EEG during visual stimulation yielded reversed attention
527 effects in the same dataset. Our findings encourage a careful and consistent choice of measures of
528 ongoing brain dynamics (here power) or measures of stimulus-related activity (here ITC), that should
529 be critically informed by the experimental question, when studying the effects of visuo-spatial
530 selective attention on the cortical processing of dynamic (quasi-) rhythmic visual stimulation. Again,
531 we emphasise that both common data analysis approaches taken here can be equally valid and
532 legitimate, yet they likely represent distinct neural phenomena. These can occur simultaneously, as
533 in our case, and may index distinct cortical processes that work in concert to facilitate the processing
534 of visual stimulation at attended locations.

535

536 **Competing interests**

537 The authors declare no competing interests.

538

539 **Author contributions**

540 CK designed research, performed research, analysed data and wrote the article. JG designed research

541 analysed data and wrote the article. AK, CSYB, CD and GT designed research and wrote the article.

542

543 **Data accessibility**

544 EEG data, pre-processed in Fieldtrip format, that underlie all analyses reported here and a

545 corresponding MATLAB analysis script are available on the Open Science Framework, osf.io/apsyf

546 (Keitel et al., 2017b).

547

548 **References**

549

550 Adrian ED, Matthews BH (1934) The interpretation of potential waves in the cortex. *J Physiol* 81:440-
551 471.

552 Andersen SK, Muller MM (2015) Driving steady-state visual evoked potentials at arbitrary frequencies
553 using temporal interpolation of stimulus presentation. *BMC Neurosci* 16:95.

554 Benwell CSY, Keitel C, Harvey M, Gross J, Thut G (2018) Trial-by-trial co-variation of pre-stimulus EEG
555 alpha power and visuospatial bias reflects a mixture of stochastic and deterministic effects.
556 *Eur J Neurosci* 48:2566-2584.

557 Benwell CSY, Tagliabue CF, Veniero D, Cecere R, Savazzi S, Thut G (2017) Prestimulus EEG Power
558 Predicts Conscious Awareness But Not Objective Visual Performance. *eNeuro* 4.

559 Blaser E, Pylyshyn ZW, Holcombe AO (2000) Tracking an object through feature space. *Nature*
560 408:196-199.

561 Bonnefond M, Jensen O (2012) Alpha oscillations serve to protect working memory maintenance
562 against anticipated distracters. *Curr Biol* 22:1969-1974.

563 Buracas GT, Zador AM, DeWeese MR, Albright TD (1998) Efficient discrimination of temporal patterns
564 by motion-sensitive neurons in primate visual cortex. *Neuron* 20:959-969.

565 Capilla A, Pazo-Alvarez P, Darriba A, Campo P, Gross J (2011) Steady-state visual evoked potentials
566 can be explained by temporal superposition of transient event-related responses. *PLoS One*
567 6:e14543.

- 568 Capilla A, Schoffelen J-M, Paterson G, Thut G, Gross J (2012) Dissociated α -Band Modulations in the
569 Dorsal and Ventral Visual Pathways in Visuospatial Attention and Perception. *Cerebral*
570 *Cortex*.
- 571 Chou EP, Hsu SM (2018) Cosine similarity as a sample size-free measure to quantify phase clustering
572 within a single neurophysiological signal. *J Neurosci Methods* 295:111-120.
- 573 Cohen MX (2014) *Analyzing neural time series data: theory and practice*. Cambridge, Massachusetts:
574 MIT Press.
- 575 Colon E, Nozaradan S, Legrain V, Mouraux A (2012) Steady-state evoked potentials to tag specific
576 components of nociceptive cortical processing. *Neuroimage* 60:571-581.
- 577 Courtemanche R, Fujii N, Graybiel AM (2003) Synchronous, focally modulated beta-band oscillations
578 characterize local field potential activity in the striatum of awake behaving monkeys.
579 *Journal of Neuroscience* 23:11741-11752.
- 580 Covic A, Keitel C, Porcu E, Schroger E, Muller MM (2017) Audio-visual synchrony and spatial attention
581 enhance processing of dynamic visual stimulation independently and in parallel: A
582 frequency-tagging study. *Neuroimage* 161:32-42.
- 583 Crosse MJ, Butler JS, Lalor EC (2015) Congruent Visual Speech Enhances Cortical Entrainment to
584 Continuous Auditory Speech in Noise-Free Conditions. *J Neurosci* 35:14195-14204.
- 585 Delorme A, Makeig S (2004) EEGLAB: an open source toolbox for analysis of single-trial EEG dynamics
586 including independent component analysis. *J Neurosci Methods* 134:9-21.
- 587 Ferree TC (2006) Spherical splines and average referencing in scalp electroencephalography. *Brain*
588 *Topogr* 19:43-52.
- 589 Freunberger R, Fellinger R, Sauseng P, Gruber W, Klimesch W (2009) Dissociation between phase-
590 locked and nonphase-locked alpha oscillations in a working memory task. *Hum Brain Mapp*
591 30:3417-3425.
- 592 Groppe DM, Bickel S, Keller CJ, Jain SK, Hwang ST, Harden C, Mehta AD (2013) Dominant frequencies
593 of resting human brain activity as measured by the electrocorticogram. *Neuroimage*
594 79:223-233.
- 595 Gross J (2014) Analytical methods and experimental approaches for electrophysiological studies of
596 brain oscillations. *J Neurosci Methods* 228:57-66.
- 597 Gross J, Pollok B, Dirks M, Timmermann L, Butz M, Schnitzler A (2005) Task-dependent oscillations
598 during unimanual and bimanual movements in the human primary motor cortex and SMA
599 studied with magnetoencephalography. *Neuroimage* 26:91-98.
- 600 Gulbinaite R, Roozendaal D, VanRullen R (2019) Attention differentially modulates the amplitude of
601 resonance frequencies in the visual cortex. *bioRxiv*.

- 602 Gulbinaite R, van Viegen T, Wieling M, Cohen MX, VanRullen R (2017) Individual Alpha Peak
603 Frequency Predicts 10 Hz Flicker Effects on Selective Attention. *J Neurosci* 37:10173-10184.
- 604 Haegens S, Zion Golumbic E (2018) Rhythmic facilitation of sensory processing: A critical review.
605 *Neurosci Biobehav Rev* 86:150-165.
- 606 Hauswald A, Lithari C, Collignon O, Leonardelli E, Weisz N (2018) A Visual Cortical Network for
607 Deriving Phonological Information from Intelligible Lip Movements. *Curr Biol* 28:1453-1459
608 e1453.
- 609 Herring JD, Thut G, Jensen O, Bergmann TO (2015) Attention Modulates TMS-Locked Alpha
610 Oscillations in the Visual Cortex. *J Neurosci* 35:14435-14447.
- 611 Herrmann CS (2001) Human EEG responses to 1-100 Hz flicker: resonance phenomena in visual
612 cortex and their potential correlation to cognitive phenomena. *Exp Brain Res* 137:346-353.
- 613 Herrmann CS, Munk MH, Engel AK (2004) Cognitive functions of gamma-band activity: memory
614 match and utilization. *Trends Cogn Sci* 8:347-355.
- 615 Iemi L, Chaumon M, Crouzet SM, Busch NA (2017) Spontaneous Neural Oscillations Bias Perception
616 by Modulating Baseline Excitability. *J Neurosci* 37:807-819.
- 617 JASP-Team (2018) JASP. In, 0.8.2 Edition.
- 618 Jensen O, Mazaheri A (2010) Shaping functional architecture by oscillatory alpha activity: gating by
619 inhibition. *Front Hum Neurosci* 4:186.
- 620 Kashiwase Y, Matsumiya K, Kuriki I, Shioiri S (2012) Time courses of attentional modulation in neural
621 amplification and synchronization measured with steady-state visual-evoked potentials. *J*
622 *Cogn Neurosci* 24:1779-1793.
- 623 Kayser J, Tenke CE (2015) On the benefits of using surface Laplacian (current source density)
624 methodology in electrophysiology. *Int J Psychophysiol* 97:171-173.
- 625 Keitel A, Gross J (2016) Individual Human Brain Areas Can Be Identified from Their Characteristic
626 Spectral Activation Fingerprints. *PLoS Biology* 14:e1002498.
- 627 Keitel C, Quigley C, Ruhnau P (2014) Stimulus-Driven Brain Oscillations in the Alpha Range:
628 Entrainment of Intrinsic Rhythms or Frequency-Following Response? *Journal of*
629 *Neuroscience* 34:10137-10140.
- 630 Keitel C, Thut G, Gross J (2017a) Visual cortex responses reflect temporal structure of continuous
631 quasi-rhythmic sensory stimulation. *Neuroimage* 146:58-70.
- 632 Keitel C, Andersen SK, Quigley C, Muller MM (2013) Independent Effects of Attentional Gain Control
633 and Competitive Interactions on Visual Stimulus Processing. *Cerebral Cortex* 23:940-946.
- 634 Keitel C, Benwell CSY, Thut G, Gross J (2017b) Alpha during quasi-periodic visual stimulation. In. *Open*
635 *Science Framework*.

- 636 Keitel C, Benwell CSY, Thut G, Gross J (2018) No changes in parieto-occipital alpha during neural
637 phase locking to visual quasi-periodic theta-, alpha-, and beta-band stimulation. *Eur J*
638 *Neurosci*.
- 639 Kelly SP, Lalor EC, Reilly RB, Foxe JJ (2006) Increases in alpha oscillatory power reflect an active
640 retinotopic mechanism for distracter suppression during sustained visuospatial attention. *J*
641 *Neurophysiol* 95:3844-3851.
- 642 Kim YJ, Grabowecky M, Paller KA, Muthu K, Suzuki S (2007) Attention induces synchronization-based
643 response gain in steady-state visual evoked potentials. *Nat Neurosci* 10:117-125.
- 644 Kizuk SA, Mathewson KE (2017) Power and Phase of Alpha Oscillations Reveal an Interaction between
645 Spatial and Temporal Visual Attention. *J Cogn Neurosci* 29:480-494.
- 646 Krancioch C (2017) Individual differences in dual-target RSVP task performance relate to
647 entrainment but not to individual alpha frequency. *PLoS One* 12:e0178934.
- 648 Lauritzen TZ, Ales JM, Wade AR (2010) The effects of visuospatial attention measured across visual
649 cortex using source-imaged, steady-state EEG. *J Vis* 10.
- 650 Lithari C, Sanchez-Garcia C, Ruhнау P, Weisz N (2016) Large-scale network-level processes during
651 entrainment. *Brain Res* 1635:143-152.
- 652 Maris E, Oostenveld R (2007) Nonparametric statistical testing of EEG- and MEG-data. *J Neurosci*
653 *Methods* 164:177-190.
- 654 Martinovic J, Andersen SK (2018) Cortical summation and attentional modulation of combined
655 chromatic and luminance signals. *Neuroimage* 176:390-403.
- 656 Mathewson KE, Prudhomme C, Fabiani M, Beck DM, Lleras A, Gratton G (2012) Making waves in the
657 stream of consciousness: entraining oscillations in EEG alpha and fluctuations in visual
658 awareness with rhythmic visual stimulation. *J Cogn Neurosci* 24:2321-2333.
- 659 Moratti S, Clementz BA, Gao Y, Ortiz T, Keil A (2007) Neural mechanisms of evoked oscillations:
660 stability and interaction with transient events. *Hum Brain Mapp* 28:1318-1333.
- 661 Morgan ST, Hansen JC, Hillyard SA (1996) Selective attention to stimulus location modulates the
662 steady-state visual evoked potential. *Proceedings of the National Academy of Sciences of*
663 *the United States of America* 93:4770-4774.
- 664 Müller MM, Teder-Sälejärvi W, Hillyard SA (1998a) The time course of cortical facilitation during cued
665 shifts of spatial attention. *Nat Neurosci* 1:631-634.
- 666 Müller MM, Picton TW, Valdes-Sosa P, Riera J, Teder-Salejarvi WA, Hillyard SA (1998b) Effects of
667 spatial selective attention on the steady-state visual evoked potential in the 20-28 Hz range.
668 *Brain Res Cogn Brain Res* 6:249-261.

- 669 Nobre AC, Rohenkohl G, Stokes M (2012) Nervous anticipation: top-down biasing across space and
670 time. In: *Cognitive Neuroscience of Attention*, 2 Edition (Posner MI, ed), pp 159-186. New
671 York: Guilford.
- 672 Nolan H, Whelan R, Reilly RB (2010) FASTER: Fully Automated Statistical Thresholding for EEG artifact
673 Rejection. *J Neurosci Methods* 192:152-162.
- 674 Norcia AM, Appelbaum LG, Ales JM, Cottareau BR, Rossion B (2015) The steady-state visual evoked
675 potential in vision research: A review. *J Vis* 15:4.
- 676 Notbohm A, Kurths J, Herrmann CS (2016) Modification of Brain Oscillations via Rhythmic Light
677 Stimulation Provides Evidence for Entrainment but Not for Superposition of Event-Related
678 Responses. *Front Hum Neurosci* 10:10.
- 679 Oostenveld R, Praamstra P (2001) The five percent electrode system for high-resolution EEG and ERP
680 measurements. *Clin Neurophysiol* 112:713-719.
- 681 Oostenveld R, Fries P, Maris E, Schoffelen JM (2011) FieldTrip: Open source software for advanced
682 analysis of MEG, EEG, and invasive electrophysiological data. *Comput Intell Neurosci*
683 2011:156869.
- 684 Park H, Kayser C, Thut G, Gross J (2016) Lip movements entrain the observers' low-frequency brain
685 oscillations to facilitate speech intelligibility. *Elife* 5.
- 686 Perrin F, Pernier J, Bertrand O, Giard MH, Echallier JF (1987) Mapping of scalp potentials by surface
687 spline interpolation. *Electroencephalogr Clin Neurophysiol* 66:75-81.
- 688 Picton TW, John MS, Purcell DW, Plourde G (2003) Human auditory steady-state responses: the
689 effects of recording technique and state of arousal. *Anesth Analg* 97:1396-1402.
- 690 Porcu E, Keitel C, Muller MM (2013) Concurrent visual and tactile steady-state evoked potentials
691 index allocation of inter-modal attention: a frequency-tagging study. *Neurosci Lett* 556:113-
692 117.
- 693 Regan D (1966) Some characteristics of average steady-state and transient responses evoked by
694 modulated light. *Electroencephalogr Clin Neurophysiol* 20:238-248.
- 695 Richter CG, Thompson WH, Bosman CA, Fries P (2015) A jackknife approach to quantifying single-trial
696 correlation between covariance-based metrics undefined on a single-trial basis.
697 *Neuroimage* 114:57-70.
- 698 Rihs TA, Michel CM, Thut G (2007) Mechanisms of selective inhibition in visual spatial attention are
699 indexed by alpha-band EEG synchronization. *Eur J Neurosci* 25:603-610.
- 700 Rouder JN, Morey RD, Speckman PL, Province JM (2012) Default Bayes factors for ANOVA designs.
701 *Journal of Mathematical Psychology* 56:356-374.

- 702 Rouder JN, Speckman PL, Sun DC, Morey RD, Iverson G (2009) Bayesian t tests for accepting and
703 rejecting the null hypothesis. *Psychonomic Bulletin & Review* 16:225-237.
- 704 Ruhnau P, Keitel C, Lithari C, Weisz N, Neuling T (2016) Flicker-Driven Responses in Visual Cortex
705 Change during Matched-Frequency Transcranial Alternating Current Stimulation. *Front Hum*
706 *Neurosci* 10:184.
- 707 Samaha J, Lemi L, Postle BR (2017) Prestimulus alpha-band power biases visual discrimination
708 confidence, but not accuracy. *Conscious Cogn* 54:47-55.
- 709 Samaha J, Bauer P, Cimaroli S, Postle BR (2015) Top-down control of the phase of alpha-band
710 oscillations as a mechanism for temporal prediction. *Proc Natl Acad Sci U S A* 112:8439-
711 8444.
- 712 Sauseng P (2012) Brain oscillations: phase-locked EEG alpha controls perception. *Curr Biol* 22:R306-
713 308.
- 714 Schoffelen JM, Oostenveld R, Fries P (2005) Neuronal coherence as a mechanism of effective
715 corticospinal interaction. *Science* 308:111-113.
- 716 Schoffelen JM, Poort J, Oostenveld R, Fries P (2011) Selective movement preparation is subserved by
717 selective increases in corticomuscular gamma-band coherence. *J Neurosci* 31:6750-6758.
- 718 Schonbrodt FD, Wagenmakers EJ (2017) Bayes factor design analysis: Planning for compelling
719 evidence. *Psychon Bull Rev*.
- 720 Spaak E, de Lange FP, Jensen O (2014) Local entrainment of alpha oscillations by visual stimuli causes
721 cyclic modulation of perception. *J Neurosci* 34:3536-3544.
- 722 Stormer VS, Alvarez GA, Cavanagh P (2014) Within-hemifield competition in early visual areas limits
723 the ability to track multiple objects with attention. *J Neurosci* 34:11526-11533.
- 724 Tallon-Baudry C, Bertrand O, Delpuech C, Pernier J (1996) Stimulus specificity of phase-locked and
725 non-phase-locked 40 Hz visual responses in human. *J Neurosci* 16:4240-4249.
- 726 Tallon-Baudry C, Bertrand O, Peronnet F, Pernier J (1998) Induced gamma-band activity during the
727 delay of a visual short-term memory task in humans. *J Neurosci* 18:4244-4254.
- 728 Thut G, Schyns PG, Gross J (2011) Entrainment of perceptually relevant brain oscillations by non-
729 invasive rhythmic stimulation of the human brain. *Front Psychol* 2:170.
- 730 Thut G, Nietzel A, Brandt SA, Pascual-Leone A (2006) Alpha-band electroencephalographic activity
731 over occipital cortex indexes visuospatial attention bias and predicts visual target detection.
732 *J Neurosci* 26:9494-9502.
- 733 van Diepen RM, Mazaheri A (2018) The Caveats of observing Inter-Trial Phase-Coherence in Cognitive
734 Neuroscience. *Sci Rep* 8:2990.

- 735 Vialatte FB, Maurice M, Dauwels J, Cichocki A (2010) Steady-state visually evoked potentials: focus on
736 essential paradigms and future perspectives. *Prog Neurobiol* 90:418-438.
- 737 Wagenmakers EJ, Wetzels R, Borsboom D, van der Maas HL (2011) Why psychologists must change
738 the way they analyze their data: the case of psi: comment on Bem (2011). *J Pers Soc Psychol*
739 100:426-432.
- 740 Walter S, Keitel C, Muller MM (2016) Sustained Splits of Attention within versus across Visual
741 Hemifields Produce Distinct Spatial Gain Profiles. *J Cogn Neurosci* 28:111-124.
- 742 Walter WG, Dovey VJ, Shipton H (1946) Analysis of the Electrical Response of the Human Cortex to
743 Photic Stimulation. *Nature* 158:540-541.
- 744 Worden MS, Foxe JJ, Wang N, Simpson GV (2000) Anticipatory biasing of visuospatial attention
745 indexed by retinotopically specific alpha-band electroencephalography increases over
746 occipital cortex. *J Neurosci* 20:RC63.
- 747 Zauner A, Fellinger R, Gross J, Hanslmayr S, Shapiro K, Gruber W, Muller S, Klimesch W (2012) Alpha
748 entrainment is responsible for the attentional blink phenomenon. *Neuroimage* 63:674-686.
- 749 Zoefel B, Ten Oever S, Sack AT (2018) The Involvement of Endogenous Neural Oscillations in the
750 Processing of Rhythmic Input: More Than a Regular Repetition of Evoked Neural Responses.
751 *Front Neurosci* 12:95.
- 752 Zumer JM, Scheeringa R, Schoffelen JM, Norris DG, Jensen O (2014) Occipital alpha activity during
753 stimulus processing gates the information flow to object-selective cortex. *PLoS Biology*
754 12:e1001965.
- 755
- 756

757 **Figure captions**

758 **Figure 1** Stimulus schematics and trial time course. **(a)** shows the time course of one trial with a cue
 759 displayed for 0.5 sec (here: Attend Right), followed by the bilateral visual stimulation for 3.5 sec. Left
 760 (L) stimulus contrast fluctuated with a rate of 10 Hz and Right (R) stimulus contrast at 12 Hz. Targets
 761 that participants were instructed to respond to were slightly altered versions of the stimuli (see
 762 inset) that were displayed occasionally for 0.3 sec. **(b)** Rhythmic visual stimulation was achieved by a
 763 frame-by-frame adjustment of global stimulus contrast (through local luminance changes) as
 764 exemplified here in one representative cycle.

765 **Figure 2** EEG spectral decomposition. **(a)** Power spectra collapsed across conditions and all electrode
 766 positions below the sagittal midline for single subjects (light grey lines) and group averages (strong
 767 black line). Note the characteristic alpha peaks in the frequency range of 8 – 13 Hz. Inset scalp map
 768 shows topographical distribution of alpha power on a dB scale based on scalp current densities. **(b)**
 769 Same as in (a) but for ‘evoked’ power. Distinct peaks are visible at stimulation frequencies 10 & 12 Hz
 770 (dashed vertical orange lines across plots). Inset scalp maps show topographical distributions of SSR
 771 power at 10 & 12 on a dB scale. Note the difference in scale between ongoing power in (a) and
 772 evoked power (b). **(c)** Same as in (a) but for inter-trial phase-locking (ITCz). Inset scalp maps show
 773 topographical distributions of SSR ITCz at 10 & 12.

774 **Figure 3** Allocation of spatial attention produces retinotopic alpha power modulation. The scalp map
 775 (top, center) depicts alpha power lateralisation (Attend Left – Attend right conditions) on a dB scale.
 776 Black dots indicate left- and right-hemispheric electrode-clusters that showed a consistent difference
 777 in group statistics (two-tailed cluster-based permutation tests). Left and right spectra illustrate alpha
 778 power differences in respective clusters when the contralateral hemifield was attended (Att) versus
 779 ignored (Ign). The bottom grey inset depicts the distribution of individual alpha power suppression
 780 effects (Ignored minus Attended) within left (L) and right (R) hemisphere clusters in the 8 – 13 Hz
 781 band. Boxplots indicate interquartile ranges (boxes) and medians (coloured vertical intersectors).
 782 Dots below show individual effects (1 dot = 1 participant).

783 **Figure 4** Attention effects on SSR evoked power (evoPow) and SSR inter-trial phase coherence. **(a)**
 784 SSR evoked power spectra show systematic power differences at the presentation frequency (10 Hz)
 785 of the left stimulus when it was attended (dark red) versus ignored (orange). The inset scalp map
 786 illustrates the topographical distribution of the attention effects. Power spectra were averaged
 787 across electrodes (black dots in scalp maps) that showed consistent attention effects in group
 788 statistics (two-tailed cluster-based permutation tests) for Attended and Ignored conditions
 789 separately. **(b)** Same as in (a) but for the 12-Hz stimulus presented in the right visual hemifield. **(c,d)**
 790 Same as in (a,b) but using ITCz as a measure of SSR inter-trial phase coherence.

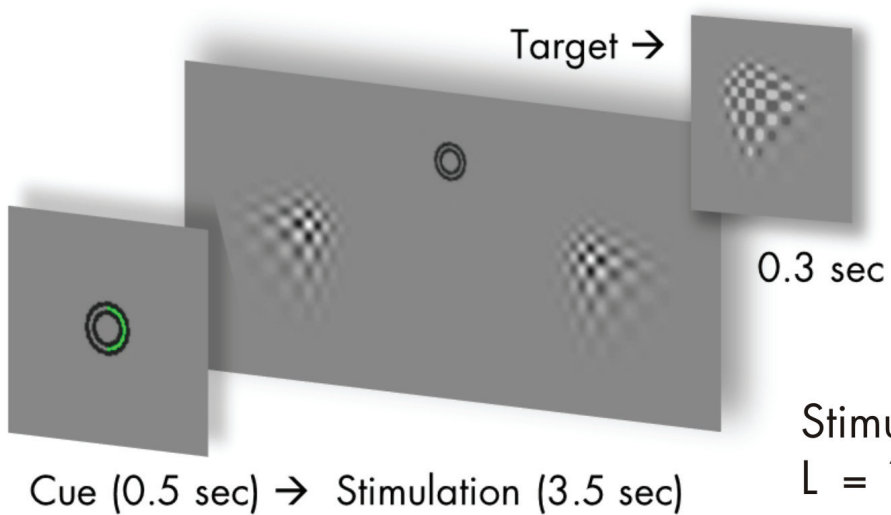
791 **Figure 5** Relationships between attention effects on alpha power and SSRs. **(a)** Individual 10-Hz (left
 792 stimulus) SSR evoked power gain (Attended minus Ignored; z-scored, y-axis) as a function of alpha
 793 suppression (Ignored minus Attended; z-scored, x axis) in overlapping left-hemispheric parieto-
 794 occipital electrode clusters. Grey dots represent participants. Coloured lines depict a straight line fit
 795 and its confidence interval (dashed lines). Goodness of fit of the linear model provided as R^2 along
 796 with corresponding P-Value. As confirmed by additional tests, both attention effects do not show a
 797 positive linear relationship that would be expected if the ipsilateral SSR power gain effect was a
 798 consequence of the ipsilateral alpha suppression. **(b)** Same as in (a), but for the 12 Hz SSR driven by
 799 the right stimulus in overlapping right-hemispheric parieto-occipital electrode clusters. **(c,d)** Similar
 800 to (a) but for attention-related gain effects on SSR ITCz (z-scored, y-axis) in (c) and gain effects on SSR
 801 evoked power in (d), both collapsed across electrode clusters showing 10- and 12-Hz SSR attention
 802 effects. Alpha suppression was collapsed across left- and right-hemispheric electrode clusters (see
 803 Figure 3).

804 **Figure 6** Summary of subject-level analysis of the linear relationship between alpha power and SSR
805 attentional modulation. **(a)** depicts the topographical distribution of group-averaged (N=17)
806 regression coefficients β (slopes) for SSR evoked power (top row) and SSR inter-trial coherence (ITC,
807 bottom row), separated by SSR frequencies 10 Hz (left column) and 12 Hz (right column). Hot colours
808 indicate a positive linear relationship and cool colours a negative relationship. Black dots in the upper
809 right panel indicate a cluster of electrodes showing a systematic effect ($p < 0.05$, cluster-based
810 permutation test) absent in tests illustrated in the other 3 panels. **(b)** Results of sensor-by-sensor
811 group-level Bayesian inference (Bayesian t-tests) of regression slopes against zero, plotted as
812 topographies on a $\log(BF_{10})$ scale. Plots arranged as in (a). Red colours indicate stronger evidence for
813 H_1 , grey colours indicate stronger evidence for H_0 . Black lines in the colour scale below scalp maps
814 denote thresholds that signal moderate evidence for H_0 ($\log(1/3) = -1.099$) or H_1 ($\log(3) = 1.099$) by
815 convention. Superimposed black dots indicate clusters showing systematic attention effects on SSR
816 evoked power / ITC as depicted in *Figure 4* for comparison.

817

a

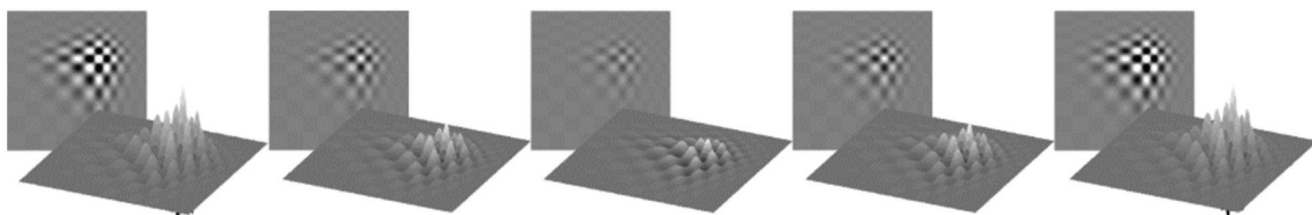
Stimulation



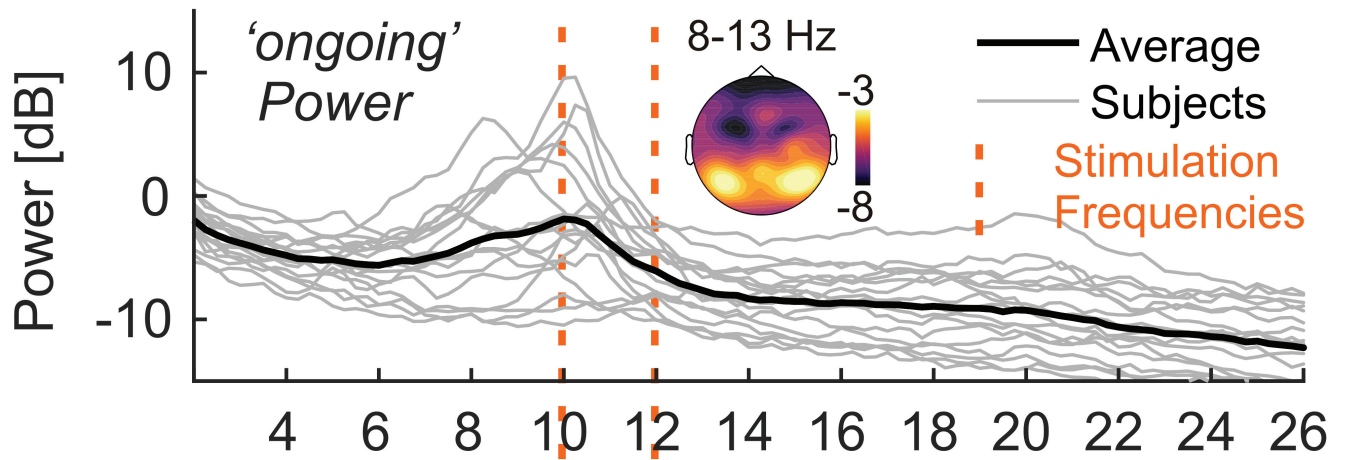
Stimulus frequency:
L = 10 Hz
R = 12 Hz

b

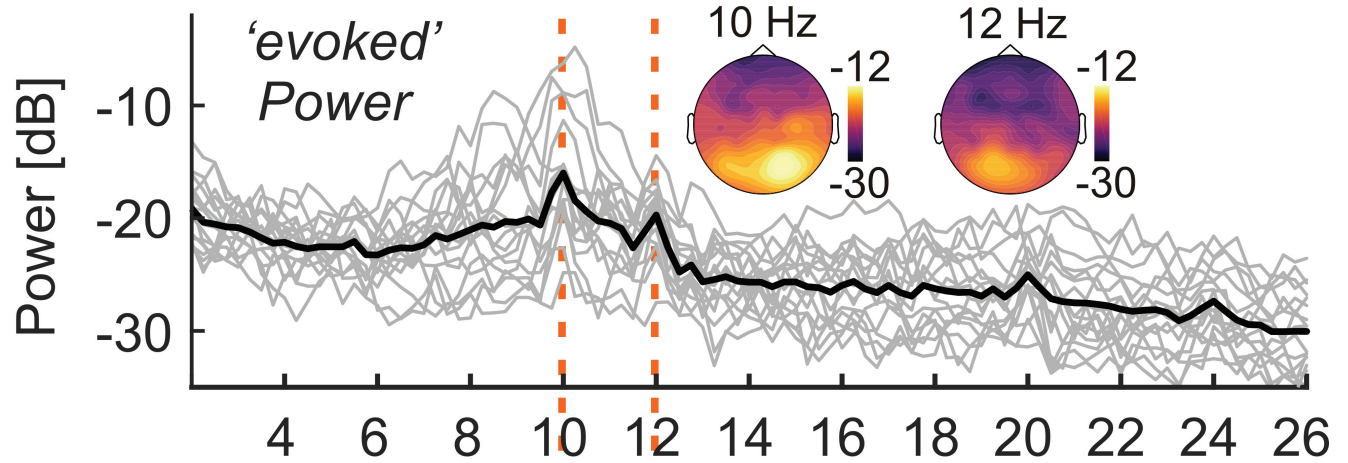
Stimulus cycle



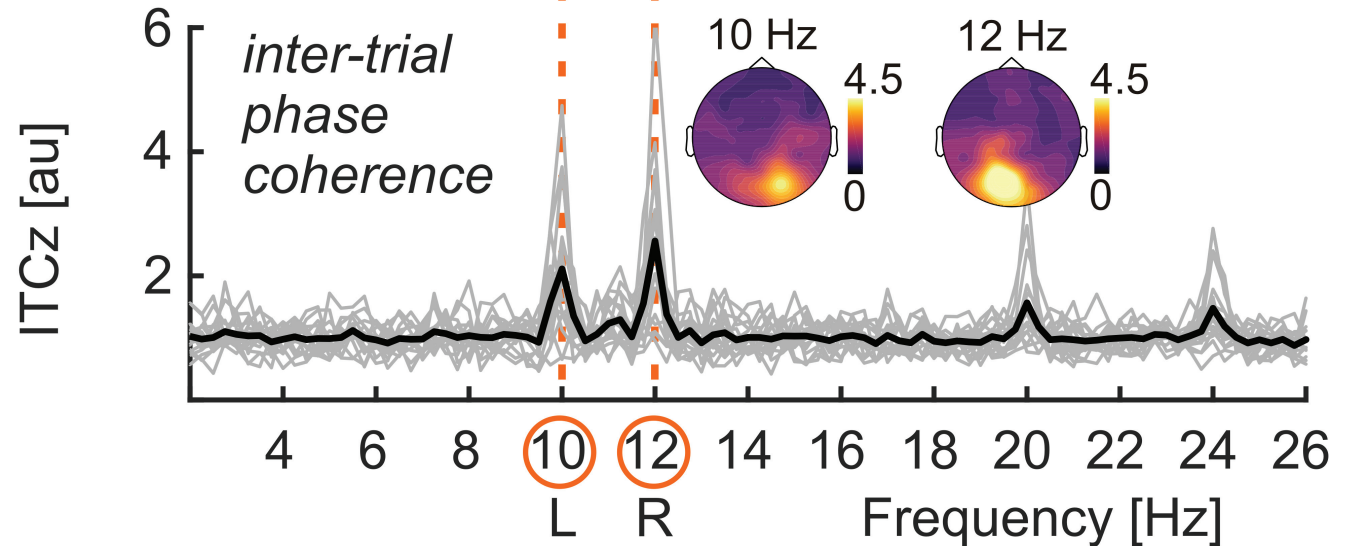
a

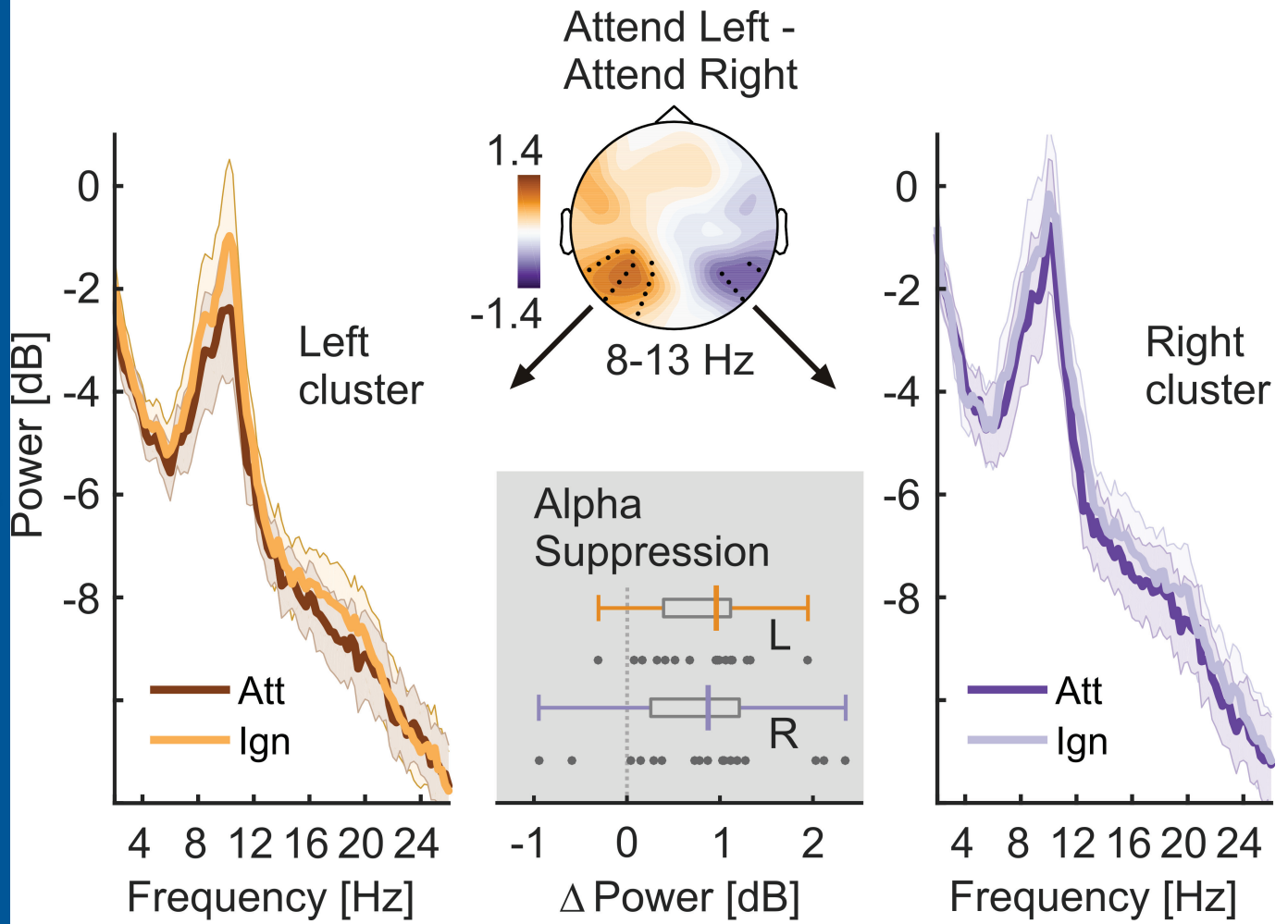


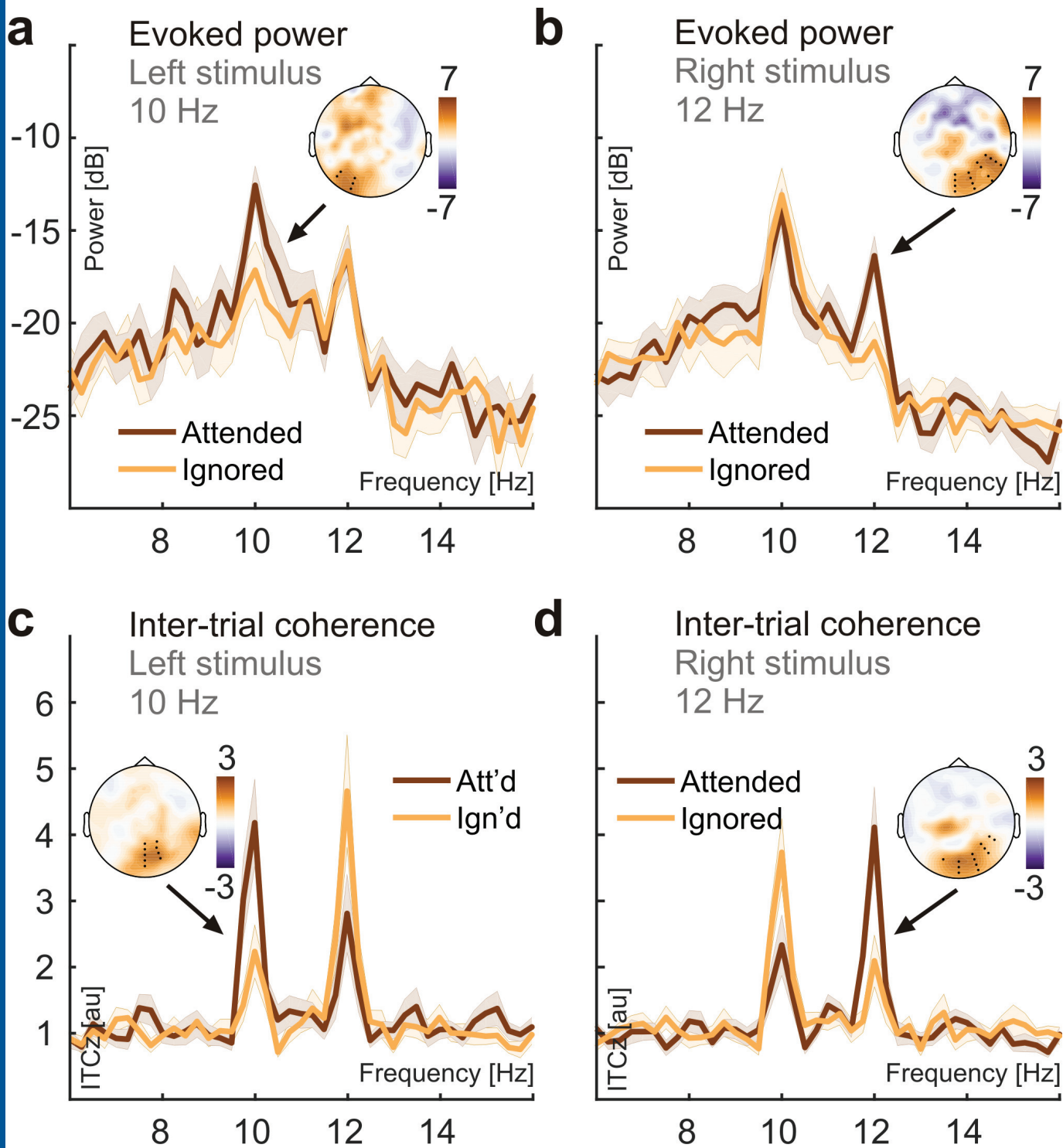
b



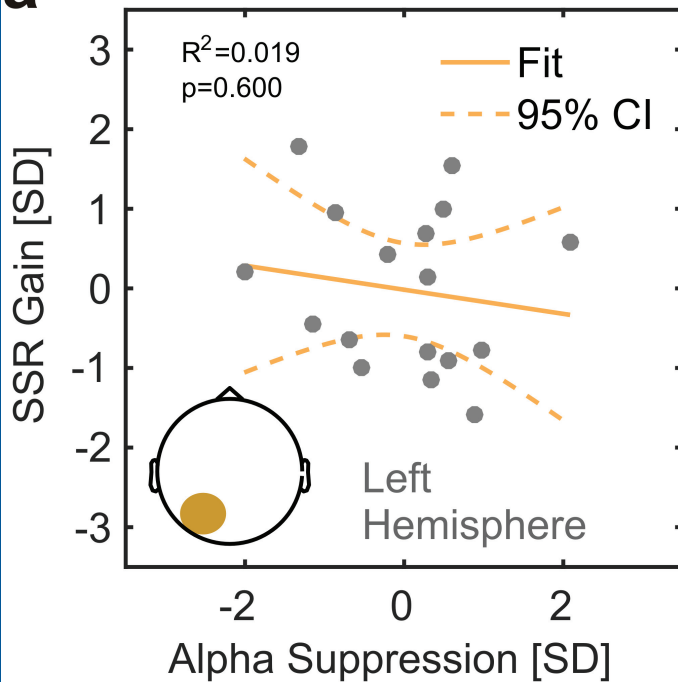
c



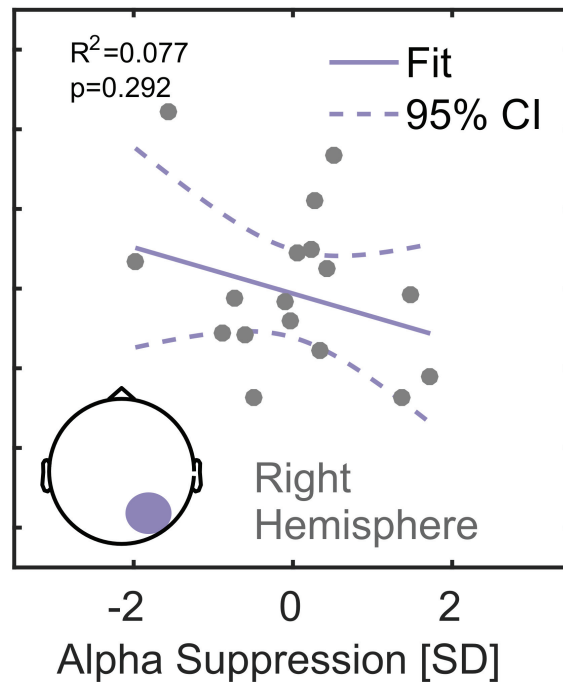




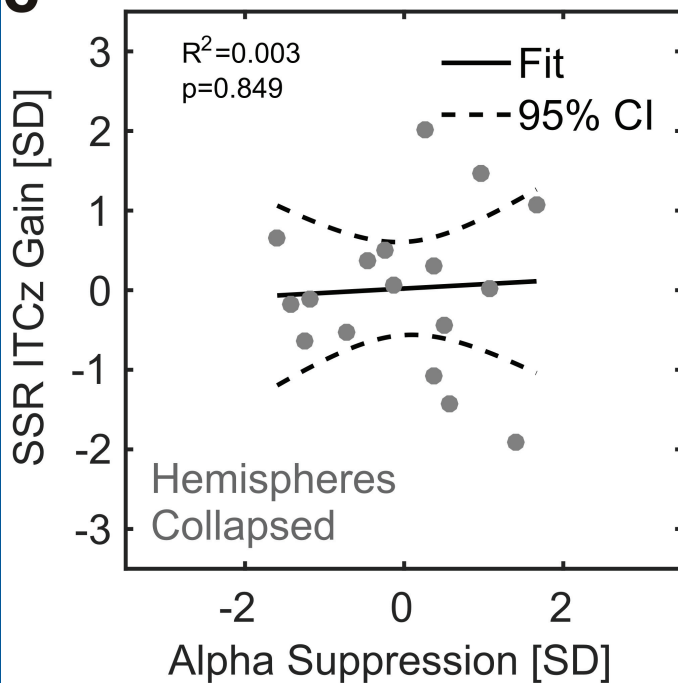
a



b



c



d

